2008-11

A review on the formation of heteronuclear cold molecules

Laser Physics, Moscow : M A I K Nauka - Interperiodica, v. 18, n. 11, p. 1305-1311, 2008
http://www.producao.usp.br/handle/BDPI/49104

ISSN 1054-660X, Laser Physics, 2008, Vol. 18, No. 11, pp. 1305–1311.

A Review on the Formation of Heteronuclear Cold Molecules

C. R. Menegatti, B. S. Marangoni, and L. G. Marcassa*

Instituto de Física de São Carlos, Universidade de São Paulo, Caixa Postal 369, São Carlos, 13560-970, SP, Brazil

*e-mail: marcassa@if.sc.usp.br

Received May 25, 2008; in final form June 1, 2008

Abstract—In this paper, we review the present status of the formation of cold ground-state heteronuclear molecules in cold-trapped atomic samples. The experimental techniques and results are presented and reviewed. The molecule production rates are compared among themselves as well as with existing theories. We conclude that theoretical and experimental improvements are necessary to help plan new experiments. The experimental results indicate that KRb and RbCs are the best systems for heteronuclear molecule production.

PACS numbers: 32.80.Rm, 37.10.Pq, 34.50.Rk

DOI: 10.1134/S1054660X08110169

INTRODUCTION

Laser cooling and trapping techniques are nowadays routinely used to produce atomic samples at temperatures around 1 mK or below. An old ambition in this field of research is the direct application of such techniques to molecules; however, due to the absence of closed-optical transitions in molecules, this is not straightforward. Therefore, new ways to cool and trap molecules should be pursued. Recently, alternative cooling and trapping schemes based on mechanical effects associated with electric–magnetic dipole moments were demonstrated, extending the ability to trap and manipulate molecules at very low temperatures [1–3]. Two main disadvantages of those techniques are the low final molecular density and the high final temperature, usually in the range of a few hundred millikelvin. Recently, ultracold homonuclear alkali metal dimers formed in magneto-optical traps (MOTs) [4–7] have emerged as reliable sources of ultracold molecules. The possibility of producing and storing cold molecular samples, at temperatures in the micro- and millikelvin range, is opening up new perspectives in chemistry, metrology, and quantum physics.

Therefore, the formation of ultracold molecules occupies a strategic position at the intersection of several powerful themes of current research in atomic and molecular physics. The understanding of the molecular formation channels within a sample of cold and trapped atoms allows for the precise determination of the scattering length, whose values are important for evaluating the stability of the Bose–Einstein condensates of alkali metal atoms [8]. Such knowledge also allows the formation of homonuclear ultracold ground-state molecules as well as its capture in optical and magnetic traps [7, 9]. Ultracold molecules should prove to be useful in spectroscopy and the study of the molecular structure, especially in ultrahigh resolution spectroscopy, which requires cold and trapped samples. Another especially promising area will be the study of collisions between ultracold molecules, in a regime where they behave like waves, perhaps giving rise to a new chemistry [10]. They may also allow for the study of collective quantum effects in molecular systems, including BECs [11]. Just like the laser cooling and trapping of neutral atoms a few years ago [12], the cooling and manipulation of cold molecules is likely to open up new branches of research. Finally, experiments to study polar molecular systems using heteronuclear molecules in order to measure the electron's permanent electric dipole moment (EDM), the lifetime of long-lived energy levels, the effects of the dipole–dipole interactions on molecular sample properties, etc. [13] have been proposed.

The investigation of the samples containing two different atomic species in the cold regime has already reached broad interest [14–16]. The KRb system has been explored in trap loss collision experiments [15, 16] and also in elastic interspecies scattering-length experiments through the measurement of the collisional rate between ^{41}K–^{87}Rb and ^{40}K–^{87}Rb [17]. Recently, the sympathetic cooling of these mixtures has lead to the achievement of the simultaneous quantum degeneracy of bosonic and fermionic species, producing BEC and Fermi–Bose mixtures [17, 18]. Due to its mass and strong long-range dispersion coefficients C_6 compared to the other heteronuclear alkali metal diatomic systems [19, 20], KRb has very favorable Franck–Condon factors for the photoassociation spectroscopy.

Electronically excited cold heteronuclear molecules were first observed in a Rb–Cs two-species magneto-optical trap (MOT) [21]. Although this was a pioneering work because it demonstrated the possibility of producing heteronuclear molecules, it presents the main disadvantage, which was the fact that the molecules were in the electronically excited state. The first cold ground-state heteronuclear molecules were observed in the KRb system by Mancini and coworkers [22] using a KRb two-species MOT. Following that paper, ground-state polar molecules were also observed in the RbCs

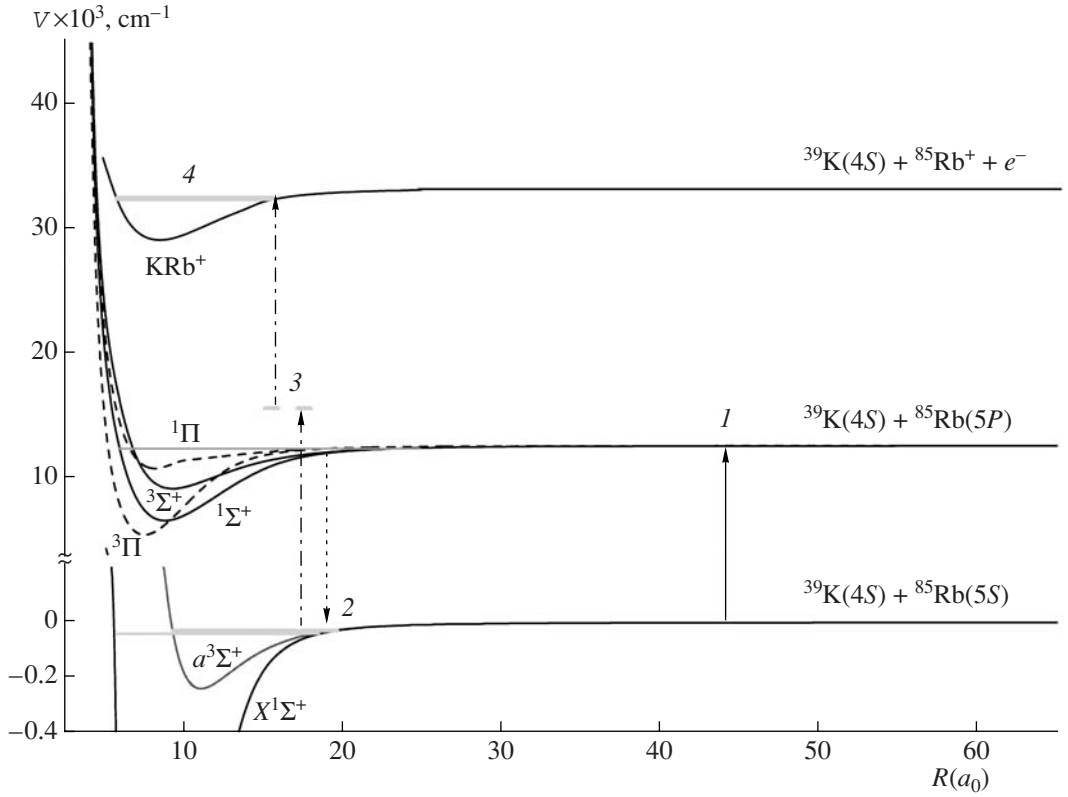

Fig. 1. Molecular formation channel for the KRb ultracold molecules and the detection channel.

system and were characterized in a detailed experiment [23, 24]. The KRb molecules were also studied experimentally in detail by Wang et al. [25]. Cold heteronuclear molecules were later also observed in the NaCs system [26] as well in the LiCs system [27]. In all of those systems, the molecules were formed by photoassociation [21–27].

However, it is also possible to produce heteronuclear molecules in the quantum degeneracy regime using the Feshbach resonances [28]. We should point out that there are two major differences between the molecules formed by photoassociation and the ones formed by Feshbach resonances in quantum systems. First, the molecules formed in the quantum regime are in the last vibrational state of the electronically ground state, the ones formed by photossociation are spread over several vibrational states. The second difference is that the photoassociated molecules are a classical gas, and the ones formed in the quantum regime are already a quantum gas. Due to such characteristics, the systems are very different from each other, and, for this reason, the molecules formed by the Feshbach resonance will not be discussed here.

In this paper, we present a review on the present status of the formation of cold ground-state heteronuclear molecules in cold-trapped atomic samples [21–27]. We start by discussing the molecule-formation channels. Then, the experimental techniques and results are reviewed. In the sequence, we present a comparison of the molecule production rates for different systems. Finally, we will compare such rates with the theoretical predictions.

MOLECULE FORMATION

Each system has it own peculiarities, but, in brief, the heteronuclear molecule formation starts with a pair of ground–ground atoms, which undergoes a quasi-resonant photon absorption. After such a transition, the pair of ground–excited atoms are attracted to each other by a long-range potential represented by a $-C_6/R^6$ interaction. In the next step, a fraction of the photoexcited molecules spontaneously decays back to the bound levels of the ground-state molecular potential after emitting a photon. The detection process is a two-photon transition using a pulsed laser, which promotes the ground-state molecules to a distribution of the bound levels of the ion molecule potential, asymptotically correlated to the dissociation limit. Finally, the ions are detected.

As an example of such a process, we have chosen to discuss the KRb molecule formation in more detail, even though the molecule formation process is very similar to other systems as well. In Fig. 1, we present a diagram illustrating the formation and detection mechanisms for the ground-state heteronuclear KRb cold

molecules. The best potential energy curves found in the literature [29, 30] for the molecular KRb were used in Fig. 1. The whole process can be represented by the following equations:

$$\mathrm{K}(4S_{1/2}) + \mathrm{Rb}(5S_{1/2}) + \hbar\omega_{\mathrm{Rb}} \longrightarrow \mathrm{K}(4S_{1/2}) + \mathrm{Rb}(5P_{3/2}) \longrightarrow \mathrm{KRb}^*(\Omega), \quad (1)$$

$$\mathrm{KRb}^*(^{1,3}\Lambda) - \hbar\omega_{\mathrm{spont}} \longrightarrow \mathrm{KRb}(^{1,3}\Sigma^+),$$

$$\mathrm{KRb}(^{1,3}\Sigma^+) + 2\hbar\omega_p \longrightarrow \mathrm{KRb}^+ + e^-. \quad (2)$$

The molecule formation starts with a pair of ground–excited atoms, attracted to each other by dispersive long-range van der Waals forces, represented by a $-C_6R^{-6}$ interaction, after undergoing the quasi-resonant absorption of a rubidium trap laser photon ω_{Rb}; KRb*(Ω) represents the excited molecular Hund's case (c) potentials with the bound levels populated at a long range by the Rb trap laser photons in step 1 (Fig. 1), and KRb*($^{1,3}\Lambda$) are the short-range excited molecular Hund's case (a) potentials ($^{1,3}\Pi$) connected to the KRb*(Ω) potentials [31]. In the next step, a fraction of the photoexcited heteronuclear molecules spontaneously decay to the bound levels of the ground-state molecular potentials KRb ($X^1\Sigma^+$ and $a^3\Sigma^+$) after emitting a photon with frequency ω_{spont} in step 2 (Fig. 1). Furthermore, the spontaneous decay rate may be enhanced by the resonant coupling between two different potential curves of the same symmetry, as suggested for the homonuclear case [32]. The detection process is a two-photon transition promoting the ground-state KRb molecules to a distribution of bound levels of the KRb^+ state potential (steps 3 and 4, Fig. 1) asymptotically correlated to the K(4S) + Rb^+ + e^- dissociation limit. This is represented by Eq. (2), where ω_p is the frequency of the ionizing pulsed-dye laser.

EXPERIMENTAL SETUP

All of the experiments involving heteronuclear cold molecules in a two-species MOT have either used a standard MOT or a dark-spot MOT (or some variation of this technique) [33]. The MOTs were loaded either from a chemical reservoir or a slow atomic beam. A combination of different lasers (dye, Ti:sapphire, and/or diode lasers) were used to trap the different atomic species (Li, Na, K, Rb, Cs) [21–27]. In typical experimental conditions, the samples are loaded with an average of 10^6–10^7 atoms, presenting maximum peak densities ranging from 10^{10} to 10^{12} cm^{-3}. The overlap between the samples was usually verified by monitoring the relative position of the atomic clouds using two charge-coupled device cameras (CCD).

The detection of the ground-state molecules was performed using pulsed-laser photoionization. The dimers formed in the trap were detected by mass spectrometry using a channel electron multiplier (channeltron) after being photoionized. A pulsed-dye laser (whose typical operation conditions were a 3–10-ns pulse duration, a 10–20-Hz repetition rate, and 1–10 mJ/pulse) provided the molecular ionization pulse. The ionization was due to a two-photon transition connecting the molecule ground state to the molecular ion state via an intermediate molecular potential. This scheme reduces the production of atomic ions. In Fig. 2a, a typical time-of-flight (TOF) spectrum for the KRb system shows the peaks due to the K_2^+, KRb^+ and Rb_2^+ ion molecules [22]. The ratio between the TOF peaks due to KRb^+ (t_{KRb}), Rb_2^+ (t_{Rb_2}), and K_2^+ (t_{K_2}) are in agreement with those based on the mass ratios (e.g., $t_{\mathrm{KRb}}/t_{\mathrm{Rb}_2} \propto \sqrt{m_{\mathrm{KRb}}/m_{\mathrm{Rb}_2}} \simeq 0.854$). To illustrate the ionization process, in Fig. 2b, we show the KRb^+ molecular ion signal as a function of the dye-laser energy per pulse. The quadratic behavior assures us that the ground-state molecules are ionized via a two-photon transition. The translational temperature of the molecules was measured by detecting the molecular ions as a function of the delay between the ionizing laser pulse and the trapping lasers switching off. Simple numerical simulation allows us to obtain the time evolution of the molecular signal and, therefore, the molecular temperature. The molecular temperatures are in agreement with the cold atomic samples from where they are produced, varying from 100 to 200 μK. In Fig. 3, we show a typical time dependence of the ion molecule signal for KRb [22], where the points are the experimental data and the full line is a theoretical fit [34]. From such data, it is possible to obtain the KRb molecular temperature, which was about 150 μK.

RESULTS AND DISCUSSION

Each molecular system presents its own peculiarity and they will be individually presented as follows.

System RbCs

In the first experiment involving RbCs, the molecules were formed in the electronically excited state [21] by photoassociation (PA). By observing trap loss in both atomic species, the authors were able to identify the RbCs bound states. Photoassociation rates as high as 10^8 s^{-1} were observed, and the authors estimated a production rate of 10^5 molecules/s in the electronically ground state. In a following work [23, 24], the authors observed the RbCs ground-state molecules by photoionization. Their atomic density (n) and atom number (N) were measured to be $n_{\mathrm{Rb}} = 7 \times 10^{11}$ cm^{-3}, $N_{\mathrm{Rb}} = 2 \times 10^8$, $n_{\mathrm{Cs}} = 1 \times 10^{12}$ cm^{-3}, and $N_{\mathrm{Cs}} = 8 \times 10^8$ for Rb and Cs, respectively. The molecules were ionized by two laser pulses, which were both 7 ns in duration and separated in time by 10 ns. The first pulse had a tunable frequency in the near infrared (IR) from 8350 to

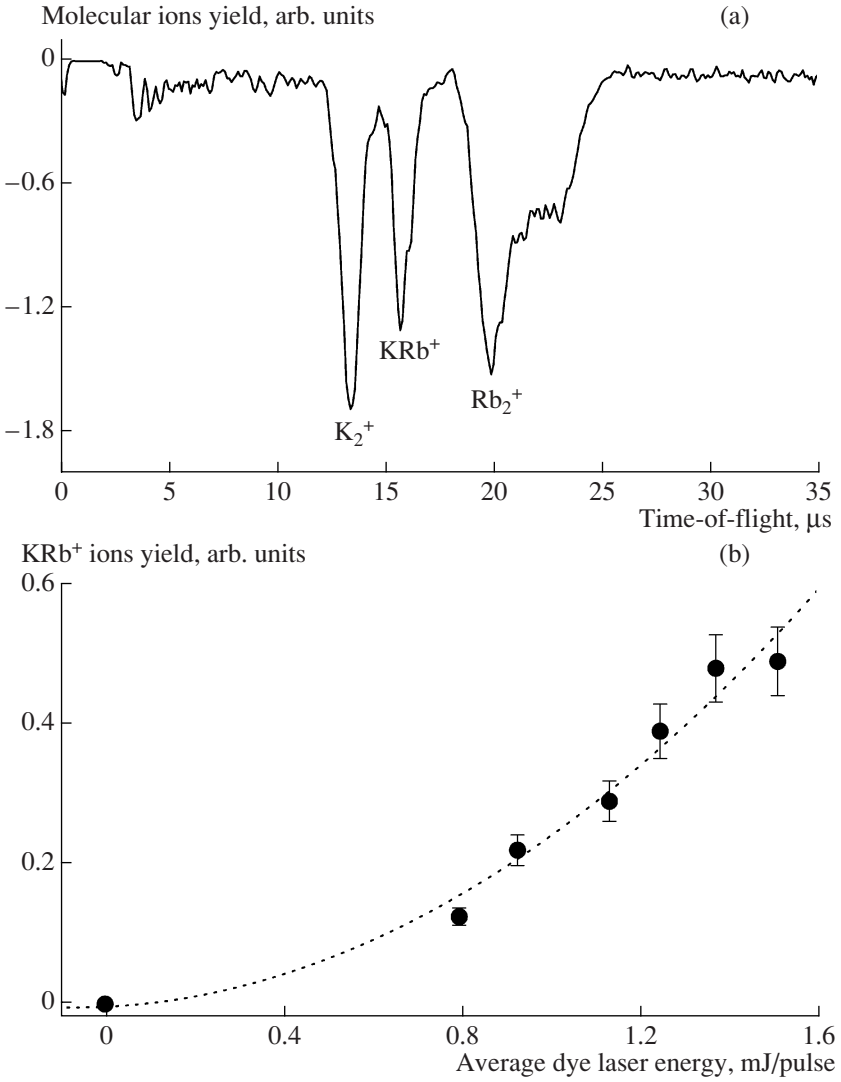

Fig. 2. (a) Typical time-of-flight (TOF) spectrum for the KRb system showing the peaks due to K_2^+, KRb^+, and Rb_2^+ ion molecules; (b) KRb^+ molecular ion signal as a function of the average dye-laser energy per pulse. The quadratic behavior assures us that the ground-state molecules are ionized via a two-photon transition.

10650 cm^{-1}. The second pulse was at 532 nm and it was generated from a Nd:Yag laser. The temperature of the molecules was estimated to be around 100 μK.

Because the photoionization efficiency is not well known, the authors have estimated under those conditions a molecule production of about 10^6 s^{-1} at a PA laser detuning around –39 cm^{-1}. It is well known that the molecule formation can be characterized by the following rate equation: $d[\mathrm{RbCs}]/dt = K_m n_{\mathrm{Rb}} n_{\mathrm{Cs}} V$, where $d[\mathrm{RbCs}]/dt$ represents the molecular signal rate, V is the intersection volume between the Rb and Cs MOTs, n_{Rb} and n_{Cs} are the atomic densities of the Rb and Cs cold samples, respectively, and K_m is the RbCs formation rate constant. For their conditions, the molecule formation rate constant may be estimated in the range 10^{-13}–10^{-12} cm^3/s.

System KRb

The first experiment to observe ground-state heteronuclear molecules was carried out by Mancini et al. [22] using a two-species MOT to trap Rb and K atoms, which were loaded from an atomic vapor. The number of trapped atoms was about 10^7 for each species with maximum peak densities of about 2×10^9 and 3×10^{10} cm^{-3} for K and Rb, respectively. The KRb molecules were produced by photoassociation due to the rubidium-trap laser beam. The detection was done by mass spectrometry using a channel electron multiplier (channeltron) after molecular photoionization. The

photoionization process was performed by a pulsed-dye laser operating at around 602.6 nm. The translational temperature was measured to be 150 μK for KRb molecules. Based on the characteristic time and amplitude response of the channeltron observed for a single molecular ion, the authors have estimated that around 100 molecules/pulse were detected. The total ion detection efficiency was 50% and the authors have considered that the ultracold molecules stayed in the trap region for a characteristic time of about 2 ms. All of these considerations have lead to a molecular formation rate of about 10^5 molecules/s and a formation rate constant of $K_m \sim 8 \times 10^{-12}$ cm^3/s.

Another experiment involving the KRb mixture was carried out by Wang et al. [25]. In this work, the authors have explored for the first time the photoassociation spectrum (PA) of a cold heteronuclear molecule, and they also demonstrated the magnetic trapping of KRb triplet ground-state molecules. Dark-spot MOTs were used to obtain typical densities of 10^{11} cm^{-3} for Rb and 3×10^{10} cm^{-3} for K. About 10–60 ions KRb^+ per laser pulse were measured when the PA laser was tuned to a strong KRb resonance (detuning around -39 cm^{-1}). The two-photon ionization was performed at 602.5 nm (1.5 mJ, ~10 ns) followed by time-of-flight mass spectroscopy. Assuming an 100% ionization efficiency for KRb and a 50% ion-detection efficiency, their maximum signal would correspond to a production rate of about 4×10^4 KRb molecules/s. For these conditions, the molecular formation rate constant may be estimated in the range 10^{-13}–10^{-12} cm^3/s.

System NaCs

Cold NaCs ground-state molecules were observed using a standard two-species vapor-cell MOT containing cold Na and Cs atoms [26]. The number of trapped atoms was 5×10^5 for Na and 2×10^6 for Cs with temperatures of 220 ± 80 μK and 210 ± 80 μK, respectively. A pulsed-dye laser (9-ns pulse duration, 20–100 μJ per pulse focused to 2 mm^2), for which the wavelength could be tuned from 575 to 600 nm, was used to ionize the ground-state molecules. At 588 nm, the authors have observed the largest $NaCs^+$ signal, which allowed them to conclude that approximately 500 NaCs ground-state molecules were observed per 10000 pulses. They also measured their translational temperature, which was determined to be 260 ± 130 μK. The authors have determined that their overall efficiency for the ionization and detection process was about 10%. Considering all of these facts and the atomic densities, they obtained a molecular formation rate of 7.4×10^{-15} cm^3/s.

System LiCs

The LiCs ground-state molecules were observed by Kraft et al. [27]. The two-species MOT was loaded from Zeeman-cooled atomic beams. There were two independent atomic sources and one Zeeman slower. This setup allowed the atomic flux to be controlled independently for each atomic species. In the MOT, the number of atoms trapped was about 10^8 for each species. The densities were 1×10^{10} cm^{-3} for Li and 5×10^9 cm^{-3} for Cs, respectively. But, due to inelastic collisions, the final number of trapped atoms was reduced to 75% of a single species. A pulsed-dye laser (7-ns pulse width, 13 mJ per pulse at 682.78 nm) provided the ionization laser beam. Considering the pulsed-laser repetition rate, detection efficiency, and ionization efficiency, the author estimated a molecule production between 1.4 ± 0.8 and 140 ± 80 s^{-1}. For these conditions, this leads to a molecular formation rate constant between 10^{-18}–10^{-16} cm^3/s.

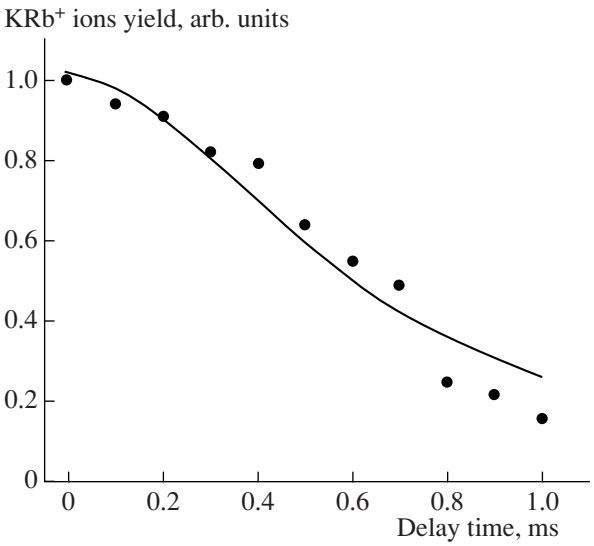

Fig. 3. Typical time dependence of the KRb^+ ion molecule signal as a function of the delay time. The points are the experimental data and the full line is a fitting [34]. From such data, it is possible to obtain the KRb molecular temperature, which was about 150 μK.

Heteronuclear Molecule Formation Rate as a Function of Mass

The results presented for all of the available heteronuclear systems are difficult to compare among themselves, because, for two experiments [23–25], the formation rates were measured for large PA-laser detunings. It is well known that the molecule production rate depends on two parameters: the free-bound Franck–Condon factor and the number of colliding pairs at a given internuclear distance, which depends on the PA-laser detuning. The Franck–Condon factor (FCF), which involves the ground-state wavefunction and the bound state of the excited state, depends on the reduced mass (μ) and the C_6 of the excited-state potential. Using a simple theory [20], it is easy to show that the relative

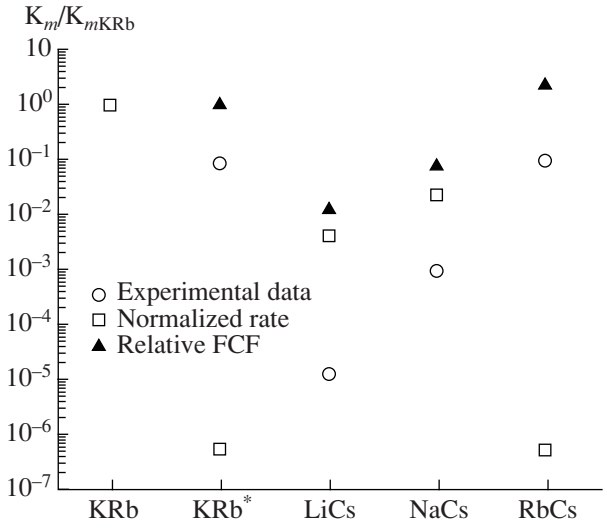

Fig. 4. Molecule production rate for all of the studied systems. In order to simplify the comparison, they were normalized for the KRb measurement of [22]. The KRb* data is from [25]. The open circles are the experimental data, the triangles are the relative Franck–Condon factor, and the open squares are the normalized molecule production rate.

Franck–Condon factor is proportional to $\mu^{9/4} C_6^{3/4}$. From such a dependence, one can conclude that the best molecules to be photoassociated are those with a larger reduced mass and the C_6 coefficient. Therefore, the best examples are KRb and RbCs.

The number of colliding pairs is proportional to $4\pi R_0^2 dR_0$, where R_0 is the distance at which photoassociation happens. In other words, R_0 is the internuclear distance at which the atomic pairs are in resonance with the PA laser and obey the resonance condition $\Delta = -C_6/hR_0^6$, where Δ is the PA-laser detuning. If we rewrite the number of colliding pairs as a function of the PA-laser detuning, we will find that it is proportional to $C_6^{1/2}/\Delta^{3/2}$. The normalized molecule production rate is the product of the Franck–Condon factor times the number of colliding pairs and, therefore, it is proportional to $\mu^{9/4} C_6^{5/4}/\Delta^{3/2}$.

In Fig. 4, we show the molecule production rate for all of the studied systems. In order to simplify the comparison, they were normalized for the KRb measurement from [22]. The open circles are the experimental data, the triangles are the relative Franck–Condon factor, and the open squares are the normalized molecule production rate as discussed previously. Our first observation is that neither the relative Franck–Condon factor or the normalized molecule production rate can predict the experimental observations. On one hand, the normalized molecule production rate fails completely to describe the experiments at large detunings, because it predicts a rate much smaller than that which is observed. On the other hand, for the LiCs and NaCs systems, it predicts a rate at least two orders of magnitude larger than the experimental results. The relative Franck–Condon factor also predicts the molecule formation rate to be at least two orders of magnitude larger. However, it predicts that the rate should increase as we go from the LiCs system to the RbCs, as observed experimentally. Clearly, the comparison of such simple theories with the experimental data is very unsatisfactory, and a more elaborate theory is necessary. We should point out that there is a more elaborate theory [35]; however, it is not valid for small laser detunings, which is the case when the PA step is performed with trapping lasers [22, 26, 27]. At small detunings, there are several problems which make the calculation of such rates very difficult. It is also important to notice that there are limitations in the experiments, especially on the determination of the photoionization efficiency and ion detection, as pointed out by all authors.

CONCLUSIONS

To summarize, we presented a review of the heteronuclear molecule formation rate measured for the RbCs, KRb, NaCs, and LiCs systems. We reviewed the formation mechanism as well as the experimental setup. We have compared the measured rates to a simple theory, and concluded that a more elaborate theory is necessary, especially at small PA-laser detunings. On the experimental side, we concluded that there are limitations, such as the two-photon transition photoionization efficiency. Undoubtedly, the experiment would benefit from some theoretical support on this issue as well. Precise knowledge of the photoionization step would produce a more trustworthy value for the molecule formation rate and, therefore, a more trustworthy comparison to the theory. This whole process would improve the theoretical–experimental comparison.

We should point out that although the simple theory from [20] has failed to predict the observed results, it was able to predict the best systems for the production of molecules by photoassociation. Since systems with a larger reduced mass and Ce coefficient are the best candidates, the KRb and RbCs systems are the natural choice. We believe that new developments in this field will happen for both systems.

ACKNOWLEDGMENTS

This work was supported by FAPESP (Fundação de Amparo à Pesquisa do Estado de São Paulo) and CNPQ.

REFERENCES

1. J. D. Weinstein, R. de Carvalho, T. Guillet, et al., Nature **395**, 148 (1998).
2. H. L. Bethlem, G. Berden, and G. Meijer, Phys. Rev. Lett. **83**, 1558 (1999).

3. J. A. Maddi, T. P. Dinneen, and H. Gould, Phys. Rev. A **60**, 3882 (1999).
4. A. Fioretti, D. Comparat, A. Crubellier, et al., Phys. Rev. Lett. **80**, 4402 (1998); A. Fioretti, D. Comparat, C. Drag, et al., Eur. Phys. J. D **5**, 389 (1999).
5. C. Gabbanini, A. Fioretti, A. Lucchesini, et al., Phys. Rev. Lett. **84**, 2814 (2000); A. Fioretti, C. Amiot, C. M. Dion, et al., Eur. Phys. J. D **15**, 189 (2001).
6. A. N. Nikolov, E. E. Eyler, X. T. Wang, et al., Phys. Rev. Lett. **82**, 703 (1999); A. N. Nikolov, J. R. Enscher, E. E. Eyler, et al., Phys. Rev. Lett. **84**, 246 (2000).
7. T. Takekoshi, B. M. Patterson, and R. J. Knize, Phys. Rev. Lett. **81**, 5105 (1998).
8. C. C. Bradley, C. A. Sackett, J. J. Tollett, and R. G. Hulet, Phys. Rev. Lett. **75**, 1687 (1995).
9. N. Vanhaecke, W. de Souza Melo, B. Laburthe Tolra, et al., Phys. Rev. Lett. **89**, 063001 (2002).
10. D. J. Heinzen, R. Wynar, P. D. Drummond, and K. V. Kheruntsyan, Phys. Rev. Lett. **84**, 5029 (2000).
11. J. Herbig, T. Kraemer, M. Mark, et al., Science **301**, 1510 (2003).
12. J. Weiner, V. S. Bagnato, S. C. Zilio, and P. Julienne, Rev. Mod. Phys. **71**, 1 (1999).
13. H. Bethlem and G. Meijer, Int. Rev. Phys. Chem. **22**, 73 (2003).
14. M. S. Santos, P. Nussenzveig, L. G. Marcassa, et al., Phys. Rev. A **52**, R4340 (1995); G. D. Telles, L. G. Marcassa, S. R. Muniz, S. G. Miranda, A. Antunes, C. Westbrook, and V. S. Bagnato, Phys. Rev. A **59**, R23 (1999); U. Schlöder, H. Engler, S. Schünemann, R. Grimm, and M. Weidemüller, Eur. Phys. J. D **7**, 331 (1999); J. P. Shaffer, W. Chalupczak, and N. P. Begelow, Phys. Rev. A **60**, R3365 (1999); Y. E. Young, R. Ejnisman, J. P. Shaffer, and N. P. Begelow, Phys. Rev. A **62**, 055403 (2000); G. D. Telles, W. Garsia, L. G. Marcassa, V. S. Bagnato, D. Ciampini, M. Fazzi, J. H. Müller, D. Wilkowski, and E. Arimondo, Phys. Rev. A **63**, 0033406 (2001).
15. L. G. Marcassa, G. D. Telles, S. R. Muniz, and V. S. Bagnato, Phys. Rev. A **63**, 013413 (2001); J. Goldwin, S. B. Papp, B. DeMarco, and D. S. Jin, Phys. Rev. A **65**, 021402(R) (2002).
16. G. Ferrari, M. Inguscio, W. Jastrzebski, et al., Phys. Rev. Lett. **89**, 053202 (2002).
17. G. Roati, F. Riboli, G. Modugno, and M. Inguscio, Phys. Rev. Lett. **89**, 150403 (2002).
18. G. Modugno, G. Ferrari, G. Roati, et al., Science **294**, 1320 (2001); G. Modugno, G. Roati, F. Riboli, et al., Science **297**, 2240 (2002).
19. M. Marinescu and H.R. Sadeghpour, Phys. Rev. A **59**, 390 (1999).
20. H. Wang and W. C. Stwalley, J. Chem. Phys. **108**, 5767 (1998).
21. A. J. Kerman, J. M. Sage, S. Sainis, et al., Phys. Rev. Lett. **92**, 033004 (2004).
22. M. W. Mancini, G. D. Telles, A. R. Caires, et al., Phys. Rev. Lett. **92**, 133203 (2004).
23. A. J. Kerman, J. M. Sage, S. Sainis, et al., Phys. Rev. Lett. **92**, 153001 (2004).
24. J. M. Sage, S. Sainis, T. Bergeman, and D. DeMille, Phys. Rev. Lett. **94**, 203001 (2005).
25. D. Wang, J. Qi, M. F. Stone, et al., Phys. Rev. Lett. **93**, 243005 (2004).
26. C. Haimberger, J. Kleinert, M. Bhattacharya, and N. P. Bigelow, Phys. Rev. A **70**, 021402(R) (2004).
27. S. D. Kraft, P. Staanum, J. Lange, et al., J. Phys. B: At. Mol. Opt. Phys. **39**, S993 (2006).
28. C. A. Stan, M. W. Zwierlein, C. H. Schunck, et al., Phys. Rev. Lett. **93**, 143001 (2004); S. Inouye, J. Goldwin, M. L. Olsen, et al., Phys. Rev. Lett. **93**, 183201 (2004).
29. S. Rousseau, A. R. Allouche, and M. Aubert-Frécon, J. Mol. Spectrosc. **203**, 235 (2000).
30. A. Valance, J. Chem. Phys. **69**, 355 (1978).
31. E. Tiemann, "Cold Molecules," in *Interactions in Ultracold Gases From Atoms to Molecules*, Ed. by M. Weidemüller and C. Zimmermann (Wiley-VCH GmbH & Co, New York, 2003).
32. C. M. Dion, C. Drag, O. Dulieu, et al., Phys. Rev. Lett. **86**, 2253 (2001).
33. W. Ketterle, K. B. Davis, M. A. Joffe, et al., Phys. Rev. Lett. **70**, 2253 (1993); C. G. Townsend, N. H. Edwards, K. P. Zetie, et al., Phys. Rev. A **53**, 1702 (1996).
34. A. Lambrecht, E. Giacobino, and S. Reynaud, Quantum Semiclassic. Opt. **8**, 458 (1996).
35. S. Azizi, M. Aymar, and O. Dulieu, Eur. Phys. J. D **31**, 195 (2004).